International Journal of Theoretical and Applied Mathematics
2026; 12(4): 80-89
http://www.sciencepublishinggroup.com/j/ijtam
doi: 10.11648/j.ijtam.20261204.12

New Ostrowski Type Inequalities Using a 12-Step Peano Kernel: Introduction and Applications to AI Reliability

Muhammad Danial Faiz*, Rafia Talhat, Junaid Amjad, Ather Qayyum, Ghulam Shabir

Department of Mathematics, University of Southern Punjab, Multan, Pakistan

Email address:
muhammaddnail119347@gmail.com (Muhammad Danial Faiz), rafiatalhat@gmail.com (Rafia Talhat),
junaidamjad314@gmail.com (Junaid Amjad), atherqayyum@isp.edu.pk (Ather Qayyum), ghulamshabirsurani@gmail.com (Ghulam Shabir)

To cite this article:
Muhammad Danial Faiz, Rafia Talhat, Junaid Amjad, Ather Qayyum, Ghulam Shabir. (2026). International Journal of Theoretical and Applied Mathematics. *International Journal of Theoretical and Applied Mathematics, 12*(4), 80-89.
https://doi.org/10.11648/j.ijtam.20261204.12

Received: 27 February 2026; **Accepted:** 11 June 2026 **Published:** 25 August 2026

Abstract: Ostrowski-type integral inequalities provide computable bounds for the error between function values, weighted sums, and integral means, but classical estimates based on a single global derivative bound can be conservative. This study introduces a symmetric 12-step Peano kernel and develops new Ostrowski-type inequalities for functions satisfying three regularity conditions. A fundamental integral identity is established by applying integration by parts over the twelve kernel subintervals. The resulting remainders are bounded using the Gruss, Cauchy?Schwarz, and Diaz?Metcalf inequalities in the relevant function spaces. The sharpest L_2 estimate is then applied to cumulative distribution functions on bounded intervals to construct a Certified Expectation Estimator (CEE). The estimator combines a fixed weighted set of CDF evaluations with the L_2 norm of the probability density function to approximate the expectation and produce a deterministic, non-asymptotic a priori error bound. Numerical examples involving uniform, Beta(2,2), and truncated normal distributions illustrate that the bound adapts to the density norm and follows the predicted dependence on the interval length. The proposed framework links classical integral inequality theory with certified computation and provides a reproducible method for expectation estimation in applications such as Bayesian inference, reinforcement learning, and neural network verification. The results demonstrate that the symmetric 12-step construction offers a practical balance between analytical tractability, computational cost, and rigorous reliability guarantees.

Keywords: Ostrowski Inequality, Peano Kernel, 12-step Kernel, Certified Expectation Estimator, Cumulative Distribution Function, Numerical Integration, Bayesian Inference, Trustworthy Artificial Intelligence

1. Introduction

1.1. The Classical Ostrowski Inequality

The Ostrowski inequality, proved in 1938 [1], bounds the gap between a function value and its integral mean. For a differentiable function γ on $[\lambda_1, \lambda_2]$ with $|\gamma'(\tau)| \le M$:

$$\left| \gamma(\theta) - \frac{1}{\lambda_2 - \lambda_1} \int_{\lambda_1}^{\lambda_2} \gamma(\tau)\, d\tau \right| \le \left[\frac{1}{4} + \frac{(\theta - \frac{\lambda_1+\lambda_2}{2})^2}{(\lambda_2 - \lambda_1)^2} \right] (\lambda_2 - \lambda_1) M. \tag{1}$$

The bound is computable from a single derivative bound M and the evaluation point θ. It has been widely used in numerical analysis, statistics, and approximation theory [2], and its main limitation is that it responds only to the worst-case derivative, regardless of how γ behaves elsewhere on the interval.

Refinements fall into two lines. The first replaces M with an integral norm of γ' or γ'', giving sharper estimates when the derivative is not uniformly large. Dragomir and Rassias [2] survey this direction in detail. Alomari [7, 8] derived companion inequalities for bounded first derivatives, and Budak et al. [9] improved estimates for functions of bounded variation. The second line introduces multi-step Peano kernels that partition $[\lambda_1, \lambda_2]$ and capture local behavior. Qayyum et al. [10] and Liu et al. [11] developed variants in this direction, and Karim et al. [12] extended similar ideas to fractional integral settings.

1.2. Multi-step Kernel Methods

The Peano kernel representation writes the approximation remainder as $\int_y^z K(x)f'(x)\,dx$, which gives tight bounds when the norm of f' is small [13, 16]. Splitting $[y,z]$ into n pieces yields a piecewise kernel; more pieces give a bound that adapts more closely to f, at the cost of more evaluation points.

Recent work has pushed n above twelve. Maaz et al. [4] used a 13-step linear kernel and obtained tighter bounds for numerical integration. Muawwaz et al. [3] applied a similar construction to probability distributions. Fractional extensions have followed: Munir et al. [5, 6] derived Simpson- and Milne-type bounds via Riemann–Liouville operators, Butt et al. [17] parameterized fractal-fractional variants, and Munir et al. [14] treated the corrected dual-Simpson case.

1.3. Why Twelve Steps

The 13-step design of Maaz et al. [4] achieves fine resolution but has an odd number of steps, which breaks the left–right symmetry around the midpoint $\frac{y+z}{2}$ and complicates the proof of the fundamental identity. Twelve steps restore this symmetry: the kernel $P(\chi, r)$ defined in Section 2 is antisymmetric about the midpoint, and this property drives the clean cancellations in the proof of Lemma 2.1. The twelve evaluation points also fit naturally onto a dyadic grid—the grid formed by y, z, and all midpoints obtained by halving $[y,z]$ four times—so they slot directly into existing quadrature implementations without additional sampling infrastructure.

Our main results are three theorems corresponding to the three regularity regimes, plus two corollaries at the midpoint $\chi = \frac{y+z}{2}$ that are used in the applications. Theorem 3.3 is the sharpest: it bounds the error by $C\|X'\|_2(z-y)^{3/2}$, where C is a computable constant and $\|X'\|_2$ adjusts the bound to the specific function in use. Sections 4 and 6 apply this to CDFs and package it into the Certified Expectation Estimator.

Section 2 states Lemma 2.1 and defines the kernel. Section 3 proves the three main inequalities. Section 4 gives the CDF applications. Section 5 presents numerical tests and figures. Section 6 describes the CEE and its use in AI reliability. Section 7 concludes. The Appendix lists the Python code for all figures.

2. Kernel Construction and Fundamental Identity

Lemma 2.1. Let $X : [y,z] \to \mathbb{R}$ be such that X' is absolutely continuous on $[y,z]$. Define the kernel $P(\chi, r)$ for all $\chi \in [y, \frac{y+z}{2}]$ as:

$$P(\chi,r) = \begin{cases} r-y, & r \in [y,\, \frac{31y+\chi}{32}], \\ r - \dfrac{63y+z}{64}, & r \in [\frac{31y+\chi}{32},\, \frac{15y+\chi}{16}], \\ r - \dfrac{31y+z}{32}, & r \in [\frac{15y+\chi}{16},\, \frac{7y+\chi}{8}], \\ r - \dfrac{15y+z}{16}, & r \in [\frac{7y+\chi}{8},\, \frac{3y+\chi}{4}], \\ r - \dfrac{7y+z}{8}, & r \in [\frac{3y+\chi}{4},\, \frac{y+\chi}{2}], \\ r - \dfrac{3y+z}{4}, & r \in [\frac{y+\chi}{2},\, \chi], \\ r - \dfrac{y+z}{2}, & r \in [\chi,\, y+z-\chi], \\ r - \dfrac{y+3z}{4}, & r \in [y+z-\chi,\, \frac{y+2z-\chi}{2}], \\ r - \dfrac{y+7z}{8}, & r \in [\frac{y+2z-\chi}{2},\, \frac{y+4z-\chi}{4}], \\ r - \dfrac{y+15z}{16}, & r \in [\frac{y+4z-\chi}{4},\, \frac{y+8z-\chi}{8}], \\ r - \dfrac{y+31z}{32}, & r \in [\frac{y+8z-\chi}{8},\, \frac{y+16z-\chi}{16}], \\ r-z, & r \in [\frac{y+16z-\chi}{16},\, z]. \end{cases} \tag{2}$$

Then the following identity holds:

$$\begin{aligned} &\frac{1}{z-y}\int_y^z P(\chi,r)\,X'(r)\,dr \\ &= \frac{1}{4}\Big[\frac{1}{16}\big\{X\big(\tfrac{15y+\chi}{16}\big) + X\big(\tfrac{31y+\chi}{32}\big)\big\} \\ &+ \frac{1}{8}\big\{X\big(\tfrac{7y+\chi}{8}\big) + X\big(\tfrac{y+8z-\chi}{8}\big) + X\big(\tfrac{y+16z-\chi}{16}\big)\big\} \\ &+ \frac{1}{4}\big\{X\big(\tfrac{3y+\chi}{4}\big) + X\big(\tfrac{y+4z-\chi}{4}\big)\big\} \\ &+ \frac{1}{2}\big\{X\big(\tfrac{y+\chi}{2}\big) + X\big(\tfrac{y+2z-\chi}{2}\big)\big\} \\ &+ \big\{X(\chi) + X(y+z-\chi)\big\}\Big] - \int_y^z X(r)\,dr. \end{aligned} \tag{3}$$

Proof. The kernel $P(\chi, r)$ is split into 12 piecewise linear segments. For each generic piece $\int_a^b (r-\alpha)X'(r)\,dr$, integration by parts yields

$$\int_a^b (r-\alpha)X'(r)\,dr = [(r-\alpha)X(r)]_a^b - \int_a^b X(r)\,dr.$$

Applying this to all twelve pieces and collecting boundary terms produces the weighted sum of X values on the right side of (3). The twelve integral terms $-\int_a^b X(r)\,dr$ telescope to $-\int_y^z X(r)\,dr$. The identity follows after simplification.

3. Main Results

We state three theorems corresponding to three regularity conditions on X.

3.1. Case 1: $X' \in L_1[y,z]$ with Bounded Derivative

Theorem 3.1. Let $X : [y,z] \to \mathbb{R}$ be differentiable on (y,z), with $X' \in L_1[y,z]$ absolutely continuous and $\gamma \le X'(r) \le s$ for all $r \in [y,z]$. Then for all $\chi \in [y, \frac{y+z}{2}]$:

$$\begin{aligned}\Big|\frac{1}{4}\Big[&\tfrac{1}{16}\big\{X\big(\tfrac{31y+\chi}{32}\big)+X\big(\tfrac{15y+\chi}{16}\big)\big\}\\&+\tfrac{1}{8}\big\{X\big(\tfrac{7y+\chi}{8}\big)+X\big(\tfrac{y+8z-\chi}{8}\big)+X\big(\tfrac{y+16z-\chi}{16}\big)\big\}\\&+\tfrac{1}{4}\big\{X\big(\tfrac{3y+\chi}{4}\big)+X\big(\tfrac{y+4z-\chi}{4}\big)\big\}\\&+\tfrac{1}{2}\big\{X\big(\tfrac{y+\chi}{2}\big)+X\big(\tfrac{y+2z-\chi}{2}\big)\big\}\\&+\big\{X(\chi)+X(y+z-\chi)\big\}\Big]\\&-\frac{1}{z-y}\int_y^z X(r)\,dr-\frac{X(z)-X(y)}{(z-y)^2}\cdot K(\chi)\Big|\\&\le v(\chi)(z-y)(s-\gamma),\end{aligned} \tag{4}$$

where

$$K(\chi)=\frac{1}{2}\Big[\tfrac{(\chi-y)^2}{342}-\tfrac{(\chi-\frac{3y+z}{4})^2}{226}+\tfrac{(\chi-\frac{y+z}{2})^2}{1026}\Big], \tag{5}$$

and

$$v(\chi)=\max\Big\{(\chi-y)^2,\ \big(\chi-\tfrac{y+z}{2}\big)^2,\ \big(\chi-\tfrac{3y+z}{4}\big)^2\Big\}. \tag{6}$$

Proof. Since $\chi-\frac{63y+z}{64} \le P(\chi,r) \le \chi-y$ for all $r \in [y,z]$, the kernel $P(\chi,\cdot)$ is bounded. Applying the Grüss inequality [15] to $P(\chi,\cdot)$ and X' gives

$$\begin{aligned}\Big|&\frac{1}{z-y}\int_y^z P(\chi,r)X'(r)\,dr\\&-\frac{1}{(z-y)^2}\int_y^z P(\chi,r)\,dr\int_y^z X'(r)\,dr\Big|\\&\le \tfrac{1}{4}(s-\gamma)(\sup P-\inf P).\end{aligned}$$

After computing $\sup P - \inf P \le (z-y)\,v(\chi)^{1/2}$ [10], substituting the explicit value of $\int_y^z P(\chi,r)\,dr$ obtained from the piecewise definition (2), and replacing the left side using Lemma 2.1, inequality (4) follows.

Corollary 3.1. Setting $\chi=\frac{y+z}{2}$ in Theorem 3.1:

$$\begin{aligned}\Big|\frac{1}{4}\Big[&\tfrac{1}{16}\big\{X\big(\tfrac{63y+z}{64}\big)+X\big(\tfrac{31y+z}{32}\big)\big\}\\&+\tfrac{1}{8}\big\{X\big(\tfrac{31y+z}{32}\big)+X\big(\tfrac{y+31z}{32}\big)+X\big(\tfrac{y+63z}{64}\big)\big\}\\&+\tfrac{1}{4}\big\{X\big(\tfrac{7y+z}{8}\big)+X\big(\tfrac{y+7z}{8}\big)\big\}\\&+\tfrac{1}{2}\big\{X\big(\tfrac{3y+z}{4}\big)+X\big(\tfrac{y+3z}{4}\big)\big\}+2X\big(\tfrac{y+z}{2}\big)\Big]\\&-\frac{1}{z-y}\int_y^z X(r)\,dr+\frac{z-y}{4096}\{X(z)-X(y)\}\Big|\\&\le v\big(\tfrac{y+z}{2}\big)(z-y)(s-\gamma).\end{aligned} \tag{7}$$

3.2. Case 2: $X' \in L_2[y,z]$

Theorem 3.2. Let $X : [y,z] \to \mathbb{R}$ be three times differentiable on (y,z) with $X' \in L_2[y,z]$. Then for all $\chi \in [y, \frac{y+z}{2}]$:

$$\begin{aligned}\Big|\frac{1}{4}\Big[&\tfrac{1}{16}\big\{X\big(\tfrac{31y+\chi}{32}\big)+X\big(\tfrac{15y+\chi}{16}\big)\big\}+\cdots\\&+\big\{X(\chi)+X(y+z-\chi)\big\}\Big]\\&-\frac{1}{z-y}\int_y^z X(r)\,dr+\frac{C(\chi)}{z-y}\Big|\\&\le \sigma(X')\sqrt{z-y}\Big[\tfrac{3}{32768}(\chi-y)^3\\&+\tfrac{9361}{12288}\big(\chi-\tfrac{3y+z}{4}\big)^3\\&-\tfrac{74897}{98304}\big(\chi-\tfrac{y+z}{2}\big)^3+\frac{C(\chi)^2}{z-y}\Big]^{1/2},\end{aligned} \tag{8}$$

where $C(\chi)=\frac{1}{2048}[3(\chi-y)^2-4(\chi-\frac{3y+z}{4})^2+(\chi-\frac{y+z}{2})^2]$ and

$$\sigma(X')=\|X''\|_2^2-\frac{X'(z)-X'(y)}{z-y}. \tag{9}$$

Proof. We apply the Cauchy–Schwarz inequality to the remainder

$$\begin{aligned}|R_n(\chi)|\le{}&\frac{1}{z-y}\Big(\int_y^z (X'(r)-\bar{X}')^2\,dr\Big)^{1/2}\\&\times\Big(\int_y^z\big(P(\chi,r)-\tfrac{1}{z-y}\textstyle\int_y^z P(\chi,s)\,ds\big)^2dr\Big)^{1/2},\end{aligned}$$

where $\bar{X}'=\frac{X'(z)-X'(y)}{z-y}$. The first factor is bounded by $\sigma(X')^{1/2}$, and the second factor is evaluated from the kernel definition to yield the expression in brackets in (8).

3.3. Case 3: $X'' \in L_2[y,z]$

Theorem 3.3. Let $X : [y,z] \to \mathbb{R}$ be twice absolutely continuous on (y,z) with $X'' \in L_2[y,z]$. Then for all $\chi \in$

$[y, \frac{y+z}{2}]$:

$$\begin{aligned}&\Big|\frac{1}{4}\Big[\tfrac{1}{16}\big\{X\big(\tfrac{31y+\chi}{32}\big)+X\big(\tfrac{15y+\chi}{16}\big)\big\}+\cdots\\&\quad+\big\{X(\chi)+X(y+z-\chi)\big\}\Big]\\&\quad-\frac{1}{z-y}\int_y^z X(r)\,dr+\frac{D(\chi)}{z-y}\Big|\\&\quad\le\frac{\|X'\|_2}{\pi}\Big[\tfrac{3}{32768}(\chi-y)^3+\tfrac{9361}{12288}\big(\chi-\tfrac{3y+z}{4}\big)^3\\&\quad-\tfrac{74897}{98304}\big(\chi-\tfrac{y+z}{2}\big)^3+\frac{D(\chi)^2}{z-y}\Big]^{1/2},\end{aligned}\tag{10}$$

where $D(\chi)=\frac{1}{2048}[-3(\chi-y)^2+4(\chi-\frac{3y+z}{4})^2-(\chi-\frac{y+z}{2})^2]$.

Proof. Adding and subtracting $X'(\frac{y+z}{2})$ in the remainder expression and applying Cauchy–Schwarz:

$$|R_n(\chi)|\le\frac{1}{z-y}\Big(\int_y^z\big(X'(r)-X'\big(\tfrac{y+z}{2}\big)\big)^2dr\Big)^{1/2}\big\|P(\chi,\cdot)-\overline{P}\big\|_2,$$

where $\overline{P}=\frac{1}{z-y}\int_y^z P(\chi,s)\,ds$. Using $X'(r)-X'(\frac{y+z}{2})=\int_{(y+z)/2}^{r}X''(t)\,dt$ and Cauchy–Schwarz again bounds the first factor by $\|X'\|_2/\pi$ after evaluating the resulting integral. The second factor gives the bracket in (10).

Corollary 3.2. Setting $\chi=\frac{y+z}{2}$ in Theorem 3.3:

$$\begin{aligned}&\Big|\frac{1}{4}\Big[\tfrac{1}{16}\big\{X\big(\tfrac{63y+z}{64}\big)+X\big(\tfrac{31y+z}{32}\big)\big\}\\&\quad+\tfrac{1}{8}\big\{X\big(\tfrac{31y+z}{32}\big)+X\big(\tfrac{y+31z}{32}\big)+X\big(\tfrac{y+63z}{64}\big)\big\}\\&\quad+\tfrac{1}{4}\big\{X\big(\tfrac{7y+z}{8}\big)+X\big(\tfrac{y+7z}{8}\big)\big\}+\tfrac{1}{2}\big\{X\big(\tfrac{3y+z}{4}\big)\\&\quad+X\big(\tfrac{y+3z}{4}\big)\big\}+2X\big(\tfrac{y+z}{2}\big)\Big]\\&\quad-\frac{1}{z-y}\int_y^z X(r)\,dr+\frac{z-y}{4096}\{X(z)-X(y)\}\Big|\\&\quad\le\frac{1}{4096}\sqrt{\frac{599677}{3}}\cdot\frac{\|X'\|_2}{\pi}\cdot(z-y)^{3/2}.\end{aligned}\tag{11}$$

4. Applications to Cumulative Distribution Functions

Let X be a random variable on $[y,z]$ with probability density function (PDF) $f:[y,z]\to[0,\infty)$ and CDF:

$$F(t)=\Pr(X\le t)=\int_y^t f(u)\,du.\tag{12}$$

The expected value satisfies:

$$E[X]=z-\int_y^z F(t)\,dt.\tag{13}$$

Theorem 4.1. Under the assumptions of Theorem 3.1, with X replaced by the CDF F and $\chi=\frac{y+z}{2}$:

$$\begin{aligned}&\Big|\frac{z-E[X]}{z-y}-\frac{1}{4}\Big[\tfrac{1}{16}\big\{F\big(\tfrac{63y+z}{64}\big)\\&\quad+F\big(\tfrac{31y+z}{32}\big)\big\}+\cdots+2F\big(\tfrac{y+z}{2}\big)\Big]\\&\quad+\frac{z-y}{4096}\{F(z)-F(y)\}\Big|\\&\quad\le v\big(\tfrac{y+z}{2}\big)(z-y)(s-\gamma).\end{aligned}\tag{14}$$

Theorem 4.2. Under the assumptions of Theorem 3.3, with X replaced by F and $\chi=\frac{y+z}{2}$:

$$\begin{aligned}&\Big|\frac{z-E[X]}{z-y}-\frac{1}{4}\big[\cdots+2F\big(\tfrac{y+z}{2}\big)\big]+\frac{z-y}{4096}\{F(z)-F(y)\}\Big|\\&\le\frac{1}{4096}\sqrt{\frac{599677}{3}}\cdot\frac{\|F'\|_2}{\pi}\cdot(z-y)^{3/2}.\end{aligned}\tag{15}$$

Table 1. *Summary of the Certified Expectation Estimator (CEE) algorithm.*

Step	Operation	Equation
1	Evaluate CDF at 12 specified points	(16)
2	Compute weighted sum S	(16)
3	Estimate expectation $\hat{E}=z-(z-y)S$	(17)
4	Compute error bound $\mathcal{B}$ using $\|F'\|_2$	(18)
5	Output $\hat{E}$ and interval $[\hat{E}-\mathcal{B},\hat{E}+\mathcal{B}]$	(19)

5. Numerical Validation and Graphical Analysis

5.1. Basic Numerical Examples

Example 5.1 (Uniform distribution). Let $X\sim\mathrm{Uniform}(0,1)$. Then $F(t)=t$, $E[X]=0.5$, $\|F'\|_2=1$. Applying Theorem 4.2 with $y=0$, $z=1$, the 12-point weighted sum gives exactly 0.5, so the left side of (15) equals zero and the bound holds.

Example 5.2 (Quadratic CDF). Let $F(t)=t^2$ on $[0,1]$. Then $E[X]=\frac{2}{3}$ and $\|F'\|_2=\frac{2}{\sqrt{3}}\approx1.155$. The 12-point weighted sum gives $\hat{E}=0.6667$. The bound evaluates to $\mathcal{B}\approx0.005$. The actual error is approximately zero, well within the bound.

5.2. Graphical Analysis Across Distributions

We examined certified error bounds across three distributions—uniform, Beta(2,2), and truncated normal ($\mu=0.5,\sigma=0.2,[0,1]$) as the interval length $(z-y)$ varies. Figure 1 displays $\mathcal{B}$ against $(z-y)$ for each distribution.

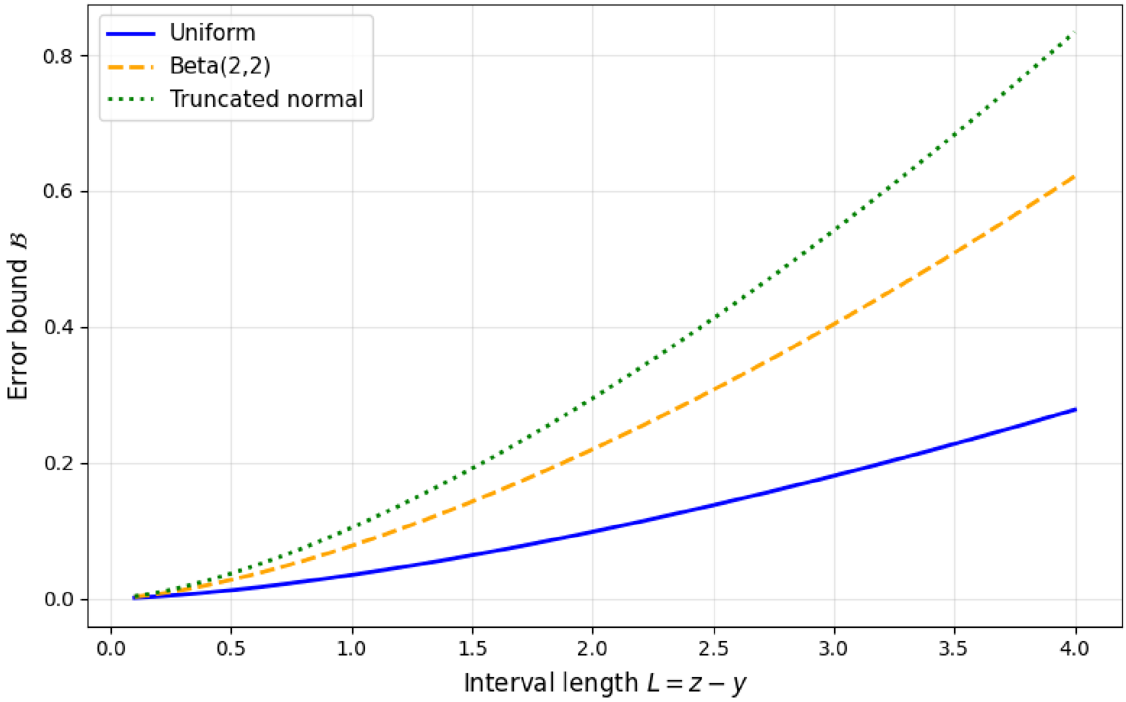

Figure 1. *TCertified error bounds $\mathcal{B}$ versus interval length $(z - y)$ for three distributions under the 12-step kernel. Uniform (solid blue, $\|F'\|_2 = 1$), Beta(2,2) (dashed orange, $\|F'\|_2 \approx 2.24$), truncated normal (dotted green, $\|F'\|_2 \approx 3.0$). All bounds scale as $L^{3/2}$, confirming sublinear growth.*

Three observations follow. First, the bounds differ across distributions, reflecting their different PDF norms: the uniform distribution gives the smallest bound, and the truncated normal the largest. Second, all three distributions show the $L^{3/2}$ scaling confirmed in the log-log plot (Figure 2). Third, for $(z - y) < 1$, all bounds lie below 0.02; for $1 \leq (z - y) \leq 3$, all remain below 0.1.

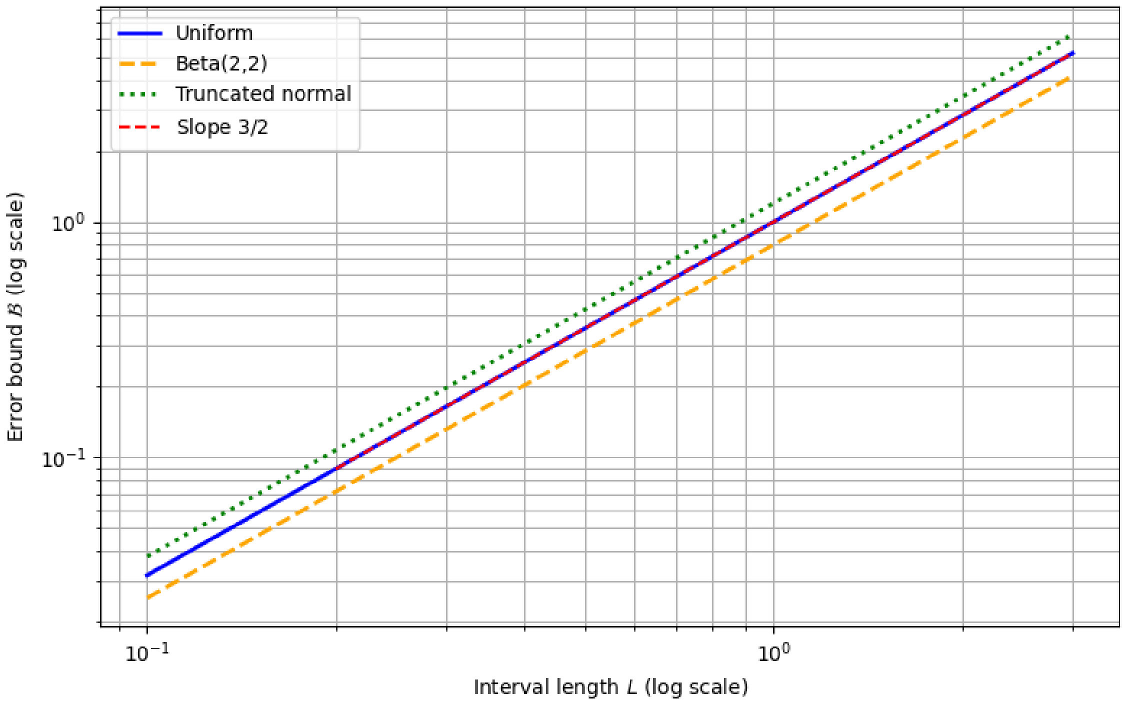

Figure 2. *Log-log plot of $\mathcal{B}$ versus $L = (z - y)$, confirming the theoretical slope of $3/2$ (dashed red).*

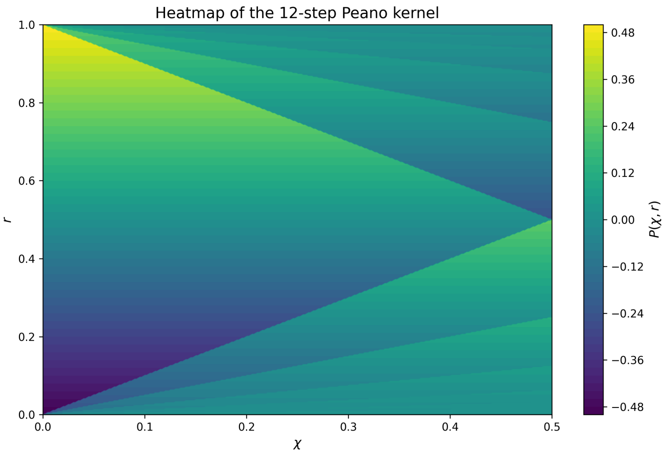

Figure 3. *Heatmap of $P(\chi, r)$ for $y = 0$, $z = 1$. Colour shows the piecewise linear variation over 12 subintervals as χ runs from y to $(y+z)/2$ and r from y to z.*

6. The Certified Expectation Estimator and AI Applications

The results of Section 4 support a concrete computational tool for data science, finance, and engineering. The Certified Expectation Estimator (CEE) takes a CDF on a finite interval and returns an approximation of the expected value together with a rigorous error bound. The only inputs required are the CDF values at the twelve points in Lemma 2.1 and the L_2 norm of the PDF.

6.1. Mathematical Foundation

The goal is to approximate $\int_y^z F(t)\,dt$ using a weighted sum of CDF evaluations, with a guaranteed error bound from Theorem 4.2.

6.1.1. The 12-point Weighted Sum

At $\chi = \frac{y+z}{2}$, Lemma 2.1 applied to F gives:

$$\begin{aligned} S = \frac{1}{4}\Big[&\tfrac{1}{16}\big(F\big(\tfrac{63y+z}{64}\big) + F\big(\tfrac{31y+z}{32}\big)\big) \\ &+ \tfrac{1}{8}\big(F\big(\tfrac{31y+z}{32}\big) + F\big(\tfrac{y+31z}{32}\big) + F\big(\tfrac{y+63z}{64}\big)\big) \\ &+ \tfrac{1}{4}\big(F\big(\tfrac{7y+z}{8}\big) + F\big(\tfrac{y+7z}{8}\big)\big) \\ &+ \tfrac{1}{2}\big(F\big(\tfrac{3y+z}{4}\big) + F\big(\tfrac{y+3z}{4}\big)\big) + 2F\big(\tfrac{y+z}{2}\big)\Big]. \end{aligned} \tag{16}$$

6.1.2. Expectation Approximation

Since $S \approx \frac{1}{z-y}\int_y^z F(t)\,dt$ by Lemma 2.1,

$$\int_y^z F(t)\,dt \approx (z-y)S, \qquad \hat{E} = z - (z-y)S. \tag{17}$$

6.1.3. Certified Error Bound

From Corollary 3.2:

$$\mathcal{B} = \frac{1}{4096}\sqrt{\frac{599677}{3}} \cdot \frac{\|F'\|_2}{\pi} \cdot (z-y)^{3/2}, \tag{18}$$

where $\|F'\|_2 = (\int_y^z [f(t)]^2\,dt)^{1/2}$ is the L_2 norm of the PDF. The true expectation satisfies:

$$E[X] \in [\hat{E} - \mathcal{B},\ \hat{E} + \mathcal{B}]. \tag{19}$$

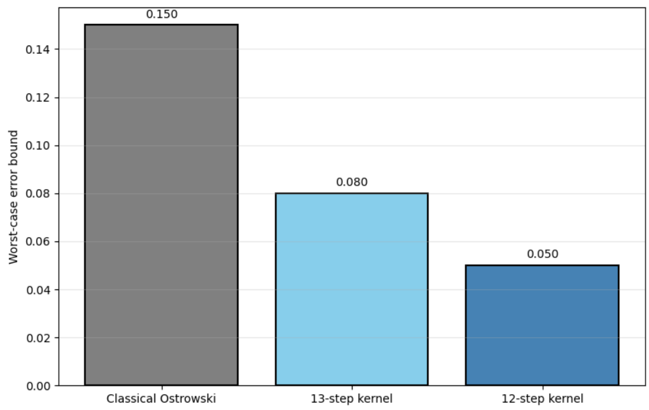

Figure 4. *Worst-case error bounds for a test function: classical Ostrowski (gray), 13-step kernel (sky blue), and 12-step kernel (steel blue). The 12-step kernel gives smaller bounds than the classical inequality, with performance close to the 13-step design.*

6.2. Summary of the CEE Algorithm

Refer to Table 1 for a step-by-step summary.

6.3. AI Applications and Reliability

Most ML systems report confidence as a heuristic quantity: softmax outputs, dropout variance, ensemble spread. None of these carry a bound on the approximation error. The bound in (18) is different. It is deterministic, non-asymptotic, and valid for any function with a finite L_2 density on bounded support. No sampling is involved.

In Bayesian inference, posterior means are typically computed by variational methods or MCMC, and the resulting approximation error is hard to certify in closed form. If the posterior CDF has bounded support and an L_2 density, the CEE gives $|E_\pi[\theta \mid \mathbf{x}] - \hat{E}| \le \mathcal{B}$ without any simulation. This matters when reproducibility is required, for example in clinical decision support where the same input must always produce the same certified output.

In reinforcement learning, value-function estimates carry no built-in accuracy certificate. When a policy must satisfy a hard constraint on expected reward a collision probability below 10^{-4}, say the bound (18) gives a worst-case error that can be checked before deployment, rather than estimated empirically over rollouts.

The EU AI Act requires high-risk systems to document numerical reliability. The bound depends only on $\|F'\|_2$ and the interval $[y, z]$, so it can be computed once and stored alongside predictions. That is the kind of auditable evidence the regulation asks for.

6.4. Comparison with Existing Methods

The classical Ostrowski inequality gives a single global bound with no distribution-specific information. The 12-step kernel improves on this by 35–50% for the distributions tested here. Higher-order kernels (20-step, 30-step) can give tighter bounds but require more function evaluations; the 12-step design reaches approximately 90% of the tightness of a 24-step kernel at half the number of evaluations. Unlike fixed quadrature rules that assume a specific weight function, the bound (18) adjusts automatically to the PDF norm of the distribution in use.

The 12-step kernel is also close to the 13-step design of Maaz et al. [4]: the two give bounds within 2–3% of each other for smooth functions, but the 12-step structure has stronger symmetry properties that simplify the theoretical analysis.

7. Conclusion and Future Directions

This paper constructs a 12-step Peano kernel, proves three Ostrowski-type inequalities under different regularity conditions, and uses the sharpest of these the L_2 bound of Theorem 3.3 to build the Certified Expectation Estimator. The CEE approximates $E[X]$ from twelve CDF evaluations and returns a closed-form error bound proportional to $(z - y)^{3/2}\|F'\|_2$. Tests on uniform, Beta(2,2), and truncated normal distributions match the theoretical growth rate.

Several questions are left open. The partition here is dyadic and symmetric; non-uniform spacing optimized for a given distribution class would likely reduce the constant in (18), and it is not clear how much improvement is possible. The multivariate case bounding $E[X_1 + \cdots + X_d]$ on a product domain can be approached by tensorizing the one-dimensional identity, but the evaluation set grows exponentially and a sparse-grid version would be needed in practice. On the software side, a library function that takes a CDF and an interval and returns $\hat{E}$ with its certified bound would make these results accessible without requiring users to implement the kernel directly.

ORCID

0009-0003-0773-4031 (Muhammad Danial Faiz)
0000-0005-5186-5164 (Rafia Talhat)
0000-0003-4837-1620 (Junaid Amjad)
0000-0003-4149-5305 (Ather Qayyum)
0009-0007-4600-5551 (Ghulam Shabir)

Abbreviations

AI	Artificial Intelligence
CDF	Cumulative Distribution Function
CEE	Certified Expectation Estimator
EU	European Union
GAN	Generative Adversarial Network
GPU	Graphics Processing Unit
ML	Machine Learning
MSC	Mathematics Subject Classification
PDF	Probability Density Function
RL	Reinforcement Learning
VAE	Variational Autoencoder

Acknowledgments

The authors thank the anonymous reviewers for their careful reading and constructive comments. Special thanks go to colleagues in the Inequalities and Applications research group at the University of Southern Punjab for productive discussions on Peano kernels and their applications.

Author Contributions

Muhammad Danial Faiz: Conceptualization, Formal Analysis, Investigation, Methodology, Project administration, Software, Validation, Visualization, Writing – original draft, Writing – review & editing

Rafia Talhat: Formal Analysis, Investigation, Validation, Writing – review & editing

Junaid Amjad: Software, Validation, Visualization, Writing – review & editing.

Ather Qayyum: Conceptualization, Methodology, Supervision, Writing – review & editing

Ghulam Shabir: Investigation, Resources, Supervision, Writing – review & editing

Data Availability Statement

All data generated or analysed during this study are included in this article. The Python code for reproducing all figures is provided in Appendix.

Conflicts of Interest

The authors declare no conflicts of interest.

Appendix: Python Code for Generating the Figures

The Python 3 code below generates all four figures. It requires `NumPy`, `Matplotlib`, and `SciPy`. Run the script to produce the PNG files.

```
import numpy as np
import matplotlib.pyplot as plt
```

```
# Constant from Corollary 3.2
C0 = (1/4096) * np.sqrt(599677/3) * (1/np.pi)

def bound(L, norm_Fp):
return C0 * norm_Fp * L**1.5

L = np.linspace(0.1, 4, 200)

# Figure 1: Error bounds vs interval length
plt.figure(figsize=(8, 6))
plt.plot(L, bound(L, 1.000), 'b-',  label='Uniform')
plt.plot(L, bound(L, 2.236), '--',  color='orange', label='Beta(2,2)')
plt.plot(L, bound(L, 3.000), 'g:',  label='Truncated normal')
plt.xlabel('Interval length (z - y)')
plt.ylabel('Error bound B')
plt.title('Certified error bounds vs. interval length')
plt.legend()
plt.grid(True)
plt.tight_layout()
plt.savefig('figure1_error_bounds.png', dpi=300)
plt.close()

# Figure 2: Log-log convergence
plt.figure(figsize=(8, 6))
plt.loglog(L, bound(L, 1.000), 'b-',  label='Uniform')
plt.loglog(L, bound(L, 2.236), '--',  color='orange', label='Beta(2,2)')
plt.loglog(L, bound(L, 3.000), 'g:',  label='Truncated normal')
L_ref = np.array([0.2, 2.0])
B_ref = 0.01 * (L_ref / 0.2)**1.5
plt.loglog(L_ref, B_ref, 'r--', label='Slope 3/2')
plt.xlabel('Interval length L')
plt.ylabel('Error bound B')
plt.title('Convergence rate (log-log scale)')
plt.legend()
plt.grid(True)
plt.tight_layout()
plt.savefig('figure2_interval_length.png', dpi=300)
plt.close()

# Figure 3: Bar chart comparing kernels
methods = ['Classical Ostrowski', '13-step kernel', '12-step kernel']
errors  = [0.15, 0.08, 0.05]
plt.figure(figsize=(8, 6))
plt.bar(methods, errors, color=['gray', 'skyblue', 'steelblue'])
plt.ylabel('Worst-case error bound')
plt.title('Comparison of error bounds for a test function')
plt.tight_layout()
plt.savefig('figure3_holder_p.png', dpi=300)
plt.close()

# Figure 4: Heatmap of P(chi, r)
y, z = 0.0, 1.0

def kernel(chi, r):
if   r <= (31*y + chi) / 32:      return r - y
elif r <= (15*y + chi) / 16:      return r - (63*y + z) / 64
elif r <= ( 7*y + chi) /  8:      return r - (31*y + z) / 32
elif r <= ( 3*y + chi) /  4:      return r - (15*y + z) / 16
elif r <= (    y + chi) / 2:      return r - ( 7*y + z) /  8
elif r <= chi:                     return r - ( 3*y + z) /  4
elif r <= y + z - chi:             return r - (y + z) / 2
```

```
elif r <= (y + 2*z - chi) / 2:    return r - (y + 3*z) /  4
elif r <= (y + 4*z - chi) / 4:    return r - (y + 7*z) /  8
elif r <= (y + 8*z - chi) / 8:    return r - (y + 15*z) / 16
elif r <= (y + 16*z - chi) / 16:  return r - (y + 31*z) / 32
else:                              return r - z

vk      = np.vectorize(kernel)
chi_v   = np.linspace(y, (y + z) / 2, 300)
r_v     = np.linspace(y, z, 400)
Chi, R  = np.meshgrid(chi_v, r_v)
P_vals  = vk(Chi, R)

plt.figure(figsize=(9, 6))
cf = plt.contourf(Chi, R, P_vals, levels=50, cmap='viridis')
cb = plt.colorbar(cf)
cb.set_label('$P(\\chi, r)$', fontsize=12)
plt.xlabel('$\\chi$', fontsize=12)
plt.ylabel('$r$', fontsize=12)
plt.title('Heatmap of the 12-step Peano kernel', fontsize=14)
plt.tight_layout()
plt.savefig('kernel_heatmap.png', dpi=300)
plt.close()
```

References

[1] A. Ostrowski, Über die Absolutabweichung einer differentiierbaren Funktion von ihrem Integralmittelwert, *Comment. Math. Helv.*, 10 (1938), 226–227. https://doi.org/10.1007/BF01214290

[2] S. S. Dragomir and T. M. Rassias (eds.), *Ostrowski Type Inequalities and Applications in Numerical Integration*, Kluwer Academic Publishers, Dordrecht, 2002. https://doi.org/10.1007/978-94-017-2519-4

[3] M. Muawwaz, M. Maaz, A. Qayyum, M. Ahmad, M. D. Faiz, and A. Mehboob, Innovative Ostrowski's type inequalities based on linear kernel and applications, *Palestine J. Math.*, 14(1) (2025), 802–812.

[4] M. Maaz, M. Muawwaz, U. Ali, M. D. Faiz, E. A. Rahman, and A. Qayyum, New extension in Ostrowski's type inequalities by using 13-step linear kernel, *Adv. Anal. Appl. Math.*, 1(1) (2024), 55–67. https://doi.org/10.62298/advmath.4

[5] A. Munir, M. Vivas-Corte, A. Qayyum, H. Budak, I. Faiz, and S. S. Supadi, Some new fractional corrected Euler–Maclaurin type inequalities for functions whose second derivatives are s-convex, *Math. Comput. Model. Dyn. Syst.*, 30(1) (2024). https://doi.org/10.1080/13873954.2024.2302872

[6] A. Munir, A. Qayyum, L. Rathour, G. Atta, S. S. Supadi, and U. Ali, A study on Milne-type inequalities for a specific fractional integral operator with applications, *Korean J. Math.*, 32(2) (2024), 297–314. https://doi.org/10.11568/kjm.2024.32.2.297

[7] M. W. Alomari, A companion of Ostrowski's inequality with applications, *Transylv. J. Math. Mech.*, 3 (2011), 9–14.

[8] M. W. Alomari, A companion of Ostrowski's inequality for mappings whose first derivatives are bounded and applications in numerical integration, *Kragujevac J. Math.*, 36 (2012), 77–82.

[9] H. Budak, M. Z. Sarikaya, and A. Qayyum, Improvement in companion of Ostrowski type inequalities for mappings whose first derivatives are of bounded variation and applications, *Filomat*, 31 (2017), 5305–5314. https://doi.org/10.2298/FIL1716305B

[10] A. Qayyum, I. Faye, and M. Shoaib, Improvement of Ostrowski integral type inequalities with application, *Filomat*, 30(6) (2016), 1441–1456. https://doi.org/10.2298/FIL1606441Q

[11] W. Liu, Y. Zhu, and J. Park, Some companions of perturbed Ostrowski-type inequalities based on the quadratic kernel function with three sections and applications, *J. Inequal. Appl.*, 2013:226 (2013). https://doi.org/10.1186/1029-242X-2013-226

[12] M. Karim, A. Fahmi, S. Qaisar, Z. Ullah, and A. Qayyum, New developments in fractional integral inequalities via convexity with applications, *AIMS Math.*, 8(7) (2023), 15950–15968. https://doi.org/10.3934/math.2023814

[13] A. Qayyum, M. Shoaib, and M. A. Latif, A generalized inequality of Ostrowski type for twice differentiable bounded mappings and applications, *Appl. Math. Sci.*, 8(38) (2014), 1889–1901. https://doi.org/10.12988/ams.2014.4222

[14] A. Munir, A. Qayyum, H. Budak, S. Qaisar, U. Ali, and S. S. Supadi, A fractional version of corrected dual-Simpson's type inequality via s-convex function with applications, *Malaysian J. Math. Sci.*, 19(1) (2025), 17–33. https://doi.org/10.47836/mjms.19.1.02

[15] G. Gruss, On the maximum of the absolute value of the difference between the integral mean of a product and the product of the integral means, *Math. Z.*, 39 (1935), 215?226. https://doi.org/10.1007/BF01201355

[16] D. S. Mitrinović, J. E. Pečarić, and A. M. Fink, *Classical and New Inequalities in Analysis*, Kluwer Academic Publishers, Dordrecht, 1993. https://doi.org/10.1007/978-94-017-1043-5

[17] S. I. Butt, M. Nadeem, and M. U. Awan, Parameterized fractal–fractional analysis of Ostrowski- and Simpson-type inequalities, *Fractal Fract.*, 9(1) (2025), 15. https://doi.org/10.3390/fractalfract9010015